Article Format: Research Article

Title: Seasonality of pCO_2 in a hard-water lake of the northern Great Plains: The legacy effects of climate and limnological conditions over 36 years.

Authors: Kerri Finlay[1*], Richard J. Vogt[2], Gavin L. Simpson[1,3], Peter R. Leavitt[1,3,4]

* Corresponding Author: Email kerri.finlay@uregina.ca. Other emails; RJV (Vogtr@yorku.ca), GLS (Gavin.Simpson@uregina.ca), PRL (Peter.Leavitt@uregina.ca)

1 Department of Biology, University of Regina, Regina, SK, S4S0A2

2 Department of Biology, York University, Toronto, ON, Canada, M3J 1P3

3 Institute of Environmental Change and Society, University of Regina, Regina, SK, S4S0A2

4 Institute for Global Food Security, Queen's University Belfast, Belfast, UK

Keywords

Lake carbon dynamics, hard-water lakes, winter ecology, seasonality, CO_2 flux, pCO_2

Running head

Regulation of seasonal pCO_2

Author Contribution Statement

KF was responsible for the conception of the manuscript, data management, and wrote the first draft of the manuscript. GLS contributed to the statistical analyses and performed the GAM analyses. RJV and PRL contributed to the direction of the analyses. All authors discussed the results and contributed to the final manuscript.

Abstract

Biogeochemical processes are active year-round in ice-covered lakes, such that processes in one season can affect limnological conditions in subsequent seasons. However, the extent and nature of these legacy effects are poorly understood, particularly for the CO_2 content of lakes and when considering gas exchange with the atmosphere. Here we used a unique 36-year dataset of weekly limnological measurements of Buffalo Pound Lake in the northern Great Plains to assess seasonal changes in CO_2 concentration and flux, and determine how dependent lake pCO_2 is on limnological conditions of previous seasons. We found that the lake was a net source of CO_2 to the atmosphere (mean 18.5 ± 7.4 mol CO_2 m^{-2} $year^{-1}$), with spring potentially accounting for the majority ($\sim 64 \pm 20\%$) of CO_2 efflux, assuming ice in spring was permeable to gas exchange ($32.9 \pm 19.8\%$ if not). Analysis with generalized additive models (GAMs) demonstrated that current and antecedent seasonal conditions combined to explain 72.6% of deviance in spring pCO_2, but that the strength of model predictions and the importance of antecedent conditions diminished in GAMs of summer (43.6%) and fall (23.3%) CO_2 levels. This research suggests that pCO_2 is regulated by a combination of coeval and historical environmental conditions, and shows that quantification of seasonal and annual fluxes requires a mechanistic understanding of the legacy effects of preceding time intervals.

Introduction

It is now well established that inland waters contribute significantly to the global carbon budget (Cole et al 2007; Prairie 2008; Tranvik et al 2009), although many questions remain about the factors regulating variability in water-column pCO_2 at broad spatial and temporal scales. One such uncertainty relates to the legacy effects of antecedent water-column conditions on current ecosystem function. For example, biogeochemical cycling under ice can substantially alter the abundance and chemical form of macronutrients in spring (Kratz et al. 1987; Hampton et al 2016) and, in the case of carbon (C), substantially increase CO_2 concentrations under ice (Kratz et al. 1987; Finlay et al. 2015). Additionally, although spring CO_2 flux has been shown to contribute significantly to total annual CO_2 flux in many lakes (Maberly 1996; Striegl et al. 2001; Ducharme-Riel et al. 2015), relatively few measurements of pCO_2 are available for shoulder seasons of summer, owing to logistical issues related to sampling during ice melt and formation. Given that lake pCO_2 is frequently elevated in spring and fall seasons relative to summer (Baehr and DeGrandpre 2002; Denfeld et al. 2015), it is important to better understand the magnitude and drivers of seasonal contributions to annual CO_2 fluxes to improve estimates of the role lakes in the global C cycle.

Seasonal variation in water-column pCO_2 in boreal lakes frequently follows predictable annual patterns of change in metabolic processes, particularly in ice-covered dimictic systems. In these lakes, CO_2 accumulates under ice in winter (Baehr and DeGrandpre 2002; Denfeld et al. 2015), causing a large efflux of CO_2 in

spring when the ice melts and the water column circulates (overturn). pCO_2 levels are reduced in summer when the water column is stable and primary production increases, while pCO_2 often increases during fall when CO_2 from respired organic matter in the hypolimnion is mixed into the water column at fall overturn (Maberly 1996; Dillon and Molot 1997; Anderson et al. 1999; Baehr and DeGrandpre 2004; Ducharme-Riel et al. 2015). Deviations from this pattern can occur due to local variation in meteorological conditions (wind, atmospheric pressure, storm runoff) which affect lake stratification and gas solubility (Vachon and del Giorgio 2014) or which introduce labile allochthonous organic matter into the lake (Lopez-Bellido et al 2012).

Less is known about seasonal patterns of pCO_2 in hardwater and saline lakes that account for nearly half of continental surface waters (Hammer 1986). In these hard-water systems, variation in pH, groundwater inputs and calcite precipitation can uncouple lake pCO_2 from metabolically-regulated processes (Striegl and Michmerhuizen 1998; Stets et al 2009; Finlay et al. 2009). Moreover, the magnitude of atmospheric CO_2 exchange in spring and fall have not been widely quantified in the shallow polymictic lakes common in agricultural lowlands, but where summer CO_2 effluxes can be much less than that seen in dimictic lakes (Finlay et al. 2009, 2015). In particular, hypolimnetic CO_2 accumulation should be relatively low in the absence of persistent thermal stratification, whereas frequent lake mixing should keep the vertical profiles of pCO_2 more uniform during the ice-free period (Anderson et al. 1999; Stets et al. 2009). Given the potential importance of such hardwater lakes in regulating atmospheric CO_2 exchange (Finlay et al. 2015), and

the predominance of spring and fall CO_2 emissions in other lakes (Ducharme-Riel et al. 2015), further research is needed on the controls of seasonal and annual CO_2 content in polymictic hardwater lakes.

Under-ice processes can be influential for many biogeochemical cycles, including that of carbon (Kratz et al. 1997), and can thus result in legacy effects where antecedent conditions propagate into subsequent seasons (Meding and Jackson 2003; Hampton et al. 2015; Powers et al. 2017). For example, respiration rates can be high under ice (Denfeld et al. 2015), particularly near the sediments where the temperature tends to be warmer than in surface waters and where organic matter accumulation is high (Wetzel 2001). Photosynthesis can also be an important control of CO_2 immediately under ice when snow cover is limited (Baehr and DeGrandpre 2002, 2004; Pernica et al. 2017). As a result, the quantity of CO_2 accumulated under ice can be a function of the duration of ice cover (Finlay et al. 2015), the availability of nutrients and light for photosynthesis (Baehr and DeGrandpre 2002, 2004; Salmi and Salonen 2016; Pernica et al. 2017), and the quantity and quality of organic matter available for mineralization (Wetzel 2001; Hampton et al. 2016). Similarly, respiratory consumption of O_2 under ice is dependent on winter conditions, as well as previous seasons' primary production (Meding and Jackson 2003). However, while biogeochemical processes during winter conditions can affect limnological conditions in spring, it is less clear how these processes affect CO_2 flux at ice-off, or whether winter legacy effects continue through summer and fall.

Together, this evidence suggests that water column pCO_2 at a given point in time is dependent on both present limnological conditions as well as those in preceding seasons. To evaluate this hypothesis, we used generalized additive models (GAMs) to quantify the magnitude and correlates of seasonal and annual CO_2 dynamics in a polymictic eutrophic hardwater lake that has been monitored year-round at weekly intervals for 36 years. Our objectives were three-fold: 1) describe seasonal variation (spring, summer, fall) in pCO_2 and potential atmospheric exchange in a polymictic lake; 2) quantify long-term (36-year) trends in CO_2 dynamics and seasonality, and 3) evaluate the influence of antecedent environmental conditions (productivity, climate) on seasonal estimates of water-column pCO_2. We predicted that spring pCO_2 would be influenced strongly by factors controlling the supply of labile organic matter and the duration of ice cover (Meding and Jackson 2003; Finlay et al. 2015), but that atmospheric CO_2 exchange in summer and fall would reflect the increasing influence of coeval meteorological and limnological conditions (Gerten and Adrian 2000; Winder and Schindler 2004). By integrating seasonal change with the importance of legacy effects, we hope to improve predictions of how future climate change may affect the contribution of lakes to the global carbon budget.

Methods

Study site

Buffalo Pound Lake is a natural lake that was impounded in 1939 and 1952 by the damming of the outflow into the Qu'Appelle River in southern Saskatchewan, Canada (Hall et al. 1999). The lake is long and narrow (1 km by 29 km), with an average depth of 3 m. The shallow depth of the lake, combined with long fetch along the prevailing storm track, results in a polymictic system that only rarely establishes weak thermal stratification (Dröscher et al. 2009).

Buffalo Pound provides the drinking water supply for the cities of Moose Jaw (population 45,000) and Regina (population 216,000), has water levels managed by the Saskatchewan Water Security Agency (SWSA), and is maintained in part by hydrologic transfer from the upstream Lake Diefenbaker reservoir (Hall et al. 1999). The lake receives runoff from a 3310 km^2 agricultural catchment area in which nutrient-rich soils favour high nutrient influx and eutrophic conditions. Although other high pH lakes in this region typically ingas CO_2 (Finlay et al. 2015), Buffalo Pound is typically oversaturated with CO_2 and exhibits net outgassing of CO_2 to the atmosphere over the last 20 years (Finlay et al. 2015).

As the main urban drinking water supply, Buffalo Pound has been monitored on a weekly basis since 1979 for 65 water quality parameters. Raw water taken from an inflow pipe 1 m above the bottom of the lake, at 3 m depth, is pumped into the water treatment plant for analyses, treatment for human use, and distribution. Measured parameters include physical (temperature), chemical (pH, nutrients, major ions), and biological (chlorophyll *a,* algae, bacteria) properties. In this study, we used measured conductivity ($\mu S\ cm^{-1}$), bicarbonate and carbonate ($mg\ L^{-1}$), pH,

and temperature (°C) to calculate pCO_2 and potential CO_2 flux. Further, we explored proxies of planktonic metabolism (Chl *a*, dissolved organic carbon [DOC]) and physico-chemical processes (water temperature, ice cover duration) as predictors of variation in pCO_2 and CO_2 fluxes across the 36-year time series

pCO_2 and CO_2 flux calculations

CO_2 concentration (μM), pCO_2 (μatm) and CO_2 flux (mmol CO_2 m^{-2} d^{-1}) were estimated for each sampling date from conductivity, water temperature and pH measurements taken from the inflow water as described in in Finlay et al. (2015). Dissolved inorganic carbon (DIC) concentrations were estimated using a previously derived relationship between measured DIC and conductivity for Buffalo Pound lake ($r^2 = 0.98$, $p<0.001$, Finlay et al 2009). Given the elevated pH of the system (average pH during the open water period = 8.3) chemically-enhanced C flux was calculated on each sampling date.

CO_2 flux was calculated as;

$$\text{net daily } CO_2 \text{ flux} = \alpha k ([CO_2]_{lake} - [CO_2]_{sat}),$$

where $[CO_2]_{lake}$ is the concentration of CO_2 in the water, $[CO_2]_{sat}$ is the concentration of CO_2 at equilibrium with the atmosphere, alpha (α) is the chemical enhancement of CO_2 flux at high pH (Hoover and Berkshire 1969), and k is piston velocity (cm h^{-1}) as determined from Model B in Vachon and Prairie (2013) relating k to wind speed and lake surface area. Hourly wind speed as measured each day at 10m height was collected from publicly available Environment Canada records for

177 the city of Moose Jaw (station 2967, http://climate.weather.gc.ca/). Flux was
178 interpolated between time points by multiplying daily flux rates by 7 days to get a
179 total potential flux for each of 52 weeks. The concentration of CO_2 at saturation with
180 the atmosphere was taken as the global mean annual CO_2 concentration measured
181 at Mauna Loa observatory.

182 Raw water was collected between 7-7:30 am, one day each week, and thus
183 diel variations in pH were not considered in this analysis. Although pH can vary
184 considerably during the day (Maberly 1996), an evaluation of continuous sonde data
185 (15 min resolution) from Buffalo Pound during summer 2014 suggested no
186 systematic bias in pCO_2 estimates due to use of morning pH measurements.
187 Specifically, pCO_2 at 7am was correlated positively with mean daily pCO_2 ($r = 0.44$,
188 $p<0.001$) and was not consistently elevated or depressed relative to the daily values.
189 Similarly, the pCO_2 values calculated from water-treatment plant samples should be
190 elevated relative to those of surface waters (Finlay et al. 2015), as water was
191 extracted 1 m above the bottom (2 m from surface) and is more affected by
192 sedimentary respiration and less by photosynthesis in this turbid system (mean
193 summer Secchi depth = 1.1 m). However, given that the lake is polymictic year-
194 round, we assumed that these surface-deep differences did not greatly influence our
195 analysis of temporal variability and causal relationships, at least during the open
196 water period (Finlay et al. 2015).

Ice-on and ice-off dates were provided by the Buffalo Pound water treatment plant and were determined as the day of year when the lake was 90% covered with ice (ice-on) or 90% ice free (for ice-off).

Definition of seasons

As the goal of this study was to quantify the magnitude of variation in seasonal pCO_2, identify potential controls thereof, and evaluate the importance of antecedent seasonal conditions on observed CO_2, we needed to establish functional definitions to delineate seasons, which accounted for inter-annual variation in winter severity and ice cover duration. Complete ice melt can take weeks and may vary with spring meteorology (Finlay et al. 2015), so we defined seasons based on a combination of potential gas exchange with the atmosphere (winter, spring) and consistent static calendar dates (summer, fall) that define when CO_2 concentrations were stable, as recommended by Anderson et al. (1999).

Herein, winter was defined as the period when the lake was completely covered with ice, and atmospheric gas exchange was negligible, beginning with the date of ice formation in the fall and continuing until the date of maximum modeled CO_2 concentration in Buffalo Pound (see below). The start of spring was defined as the date when CO_2 concentrations begin to decline, assuming that this pattern arises from loss of CO_2 to the atmosphere (see Discussion), even if this occurred before the recorded ice-off date. Spring continued until the minimum CO_2 concentration was recorded (within 100 days of CO_2 maxima). Spring was further divided into two phases for CO_2 flux analyses: “potential spring”, which was defined as the period of

time between maximum CO_2 concentration and ice-off date; and "open-water spring", the period from documented ice-off until the minimum CO_2 concentration. Hereafter, "spring" refers to the period that includes both "potential" and "open-water" spring periods, and annual flux rates include "potential" spring, unless otherwise indicated. Summer was then calculated as the date after the spring CO_2 minimum continuing until Aug 31 of that year, whereas fall was defined as the period from Sept 1 until ice-on, as we have done previously (Finlay et al. 2015).

Statistical Analyses

The time series of *in situ* pCO_2 was modeled using a generalized additive model (GAM) comprising terms to account for both within- and between-year variation in the time series. We chose to model the data using a GAM because this approach better accounts for non-linearity of trends relative to other protocols (e.g., Mann Kendall test) and because GAMs uniquely allow us to estimate the magnitudes of within- and between-year trends in the data, derive secondary estimates from the model (e.g., the magnitude of efflux at ice-out), and quantify uncertainties. For example, the commonly-used (seasonal) Mann Kendall test does not estimate the magnitude(s) of trends, tests only for monotonic trends (which were not indicated in preliminary data screening), and does not allow derivation of secondary estimates as above. Similarly, estimation of trends using parametric linear or generalized linear models would require us to a priori state the functional form of the within- and between-year trends in time series or perform model selection from among a set of complex polynomial models. Using GAMs, we avoid this subjective

element of model specification by allowing the functional form of the trends to be determined from the data, whilst the use of splines avoids well-known bias issues at the ends of series that plague polynomial models. Details of candidate model selection and estimates are included in the Supplementary Information.

To determine the start and end dates of spring, the best-fitting GAM for the pCO_2 time series was used to estimate annual mean differences between the minimum and maximum pCO_2 between days 50 (Feb 19) and 160 (~June 9). In this procedure, an estimate for the expected difference for each year can be derived by predicting daily pCO_2 for each day in the specified interval, finding the peak pCO_2 during the period, and calculating the difference between the two pCO_2 extremes. Of the 36 years of data collection, 4 years did not have a pronounced pCO_2 peak and those years were not included in subsequent statistical analyses. Uncertainty in the estimated pCO_2 trend was evaluated using 10,000 simulations of the trend from the posterior distribution of the fitted GAM (details in Supplementary Information).

Variables known from the literature to affect pCO_2 content of prairie hardwater lakes were selected *a priori* to develop individual GAMs for each season to predict pCO_2 in Buffalo Pound (Meding and Jackson 2003; Finlay et al. 2009, 2010). Specifically, spring CO_2 flux was expected to be dependent on ice-cover duration (longer ice cover resulting in greater accumulation of respired CO_2), and the productivity of the previous summer (providing the material for respiration over winter) approximated as Chl *a* (Meding and Jackson 2003; Finlay et al. 2015). In contrast, we expected that summer and fall pCO_2 would be more heavily

dependent on pCO_2 in the previous season and coeval limnological conditions (Finlay et al. 2009, 2010). To test these hypotheses, we developed GAMs to evaluate the effects of coeval mean water temperature, Chl *a*, DOC, and ice cover duration in the models, and examined legacy effects on seasonal lake pCO_2 by including mean values from preceding seasons. Given that not all variables were measured in all years, direct AIC comparisons were not appropriate for determining the best fitting model for each season. Instead we selected models that maximized deviance explained, adjusted R^2 (R^2_{adj}), and sample size (n), in addition to a qualitative exploration of the model fits. More details of model selection are included in the Supplementary Information.

GAMs were estimated using the mgcv package (version 1.8-22; Wood 2017), and graphics were plotted with package ggplot2 (Wickham 2009) for R (version 3.4-3; R Core Team, 2018).

Results

Estimation of pCO_2 from water chemistry suggested that Buffalo Pound Lake should outgas CO_2 during the open-water season of most years (Fig. 1). Estimates of total annual CO_2 flux (including potential spring flux) ranged from a minimum of 4.36 mol m^{-2} $year^{-1}$ in 1988 to a maximum of 41.97 mol m^{-2} $year^{-1}$in 1992, with a mean ($\pm$ SD) annual flux rate of 18.53 $\pm$ 7.38 mol m^{-2} $year^{-1}$. Instantaneous CO_2 fluxes ranged dramatically from an efflux of 886.8 mmol m^{-2} day^{-1} to an influx of 49.1 mmol m^{-2} day^{-1}. Buffalo Pound Lake also exhibited ingassing of CO_2 in summer or fall seasons of four years (1979, 1987, 1991, 2012), but none of these events

resulted in the basin experiencing a net influx of CO_2 when calculated at an annual scale. Over the entire 36-year dataset, total spring CO_2 efflux averaged 63.8% of total flux (± 19.8 %), but this value declines to 32.9% (± 19.8%) when only open-water spring flux is considered. In contrast, CO_2 efflux was lowest in summer (14.0% of annual total), and increased slightly in fall (22.2%).

There were no pronounced decadal-scale trends in estimated CO_2 content or effluxes from Buffalo Pound Lake (Fig. 2). Seasonal averages of pCO_2 (μatm) varied by year, with spring pCO_2 being the highest, averaging 1797 μatm (range 480.1-3334 μatm), summer pCO_2 is the lowest and with less variability (average 683, range 62.3-1387 μatm), and fall intermediate between the spring and summer (average 818.9, range 327-1981μatm). Winter pCO_2 averaged 1730 μatm with a min of 499 and a max of 3687. We did not see any significant ($p > 0.1$) decadal scale trends with pCO_2 in each season vs. year (regression of data in Fig 2), or with annual pCO_2 averages vs. year.

The best-fitting GAM to model the pCO_2 time series was a tensor-product smooth of sampling date and day of year as a seasonal trend which varied smoothly with the between-year trend. This model was also the most complex in terms of the effective degrees of freedom (EDF=506.8), but provided better fit to observed data (AIC = 25769) than did the next best model (AIC = 25926). The best-fit model explained 97% of deviance in the pCO_2 data, with an adjusted R^2 of 0.90. Qualitatively, the best-fit model also better explained large annual peaks in pCO_2, as well as year-to-year variation in the magnitude of that peak. Overall, the mean pCO_2

307 estimated by the best-fit model oscillated slowly over the 36 years of study and did
308 not exhibit sudden changes between years.

309 In most years, modeled pCO_2 increased under ice, declined substantially at
310 spring ice melt, stayed low during summer, and, with a few exceptions, remained
311 low until ice formation in the fall (Fig. 3). Ice-cover duration varied >7 weeks across
312 the 36-year period, from a minimum of 133 days in 2000 to a maximum of 183 days
313 in 1979 (mean 156.7 $\pm$ 12.5 days). The length of spring CO_2 decline varied from 3
314 weeks (in 1986 and 1988) to 15 weeks (1991) with a mean ($\pm$ SD) of 10.5 ($\pm$ 2.9)
315 weeks. On average, the spring pCO_2 decline started 4.9 $\pm$ 2.3 weeks before the
316 observed date of ice melt. In contrast, there were few indications of a sudden
317 change in estimated pCO_2 in fall such as would be expected if CO_2 were released
318 suddenly from hypolimnetic waters at fall mixis (Vachon and del Giorgio 2014;
319 Ducharme-Riel et al. 2015). Instead, pCO_2 peaked during winter in most years (Fig.
320 3b), with only a few years showing limited CO_2 build-up under ice (1984, 1987,
321 1995, 2012). There were no statistically significant trends in the relationship
322 between fall pCO_2 and the timing of ice formation.

323 Comparison of GAMs developed independently for spring, summer and fall
324 seasons revealed that the influence of antecedent seasonal conditions on pCO_2
325 declined from spring to fall (Fig. 4, Supplementary Information). For example, the
326 best fit GAM for spring pCO_2 used the scaled t distribution for heavily tailed data and
327 explained 72.6% of the deviance (R^2_{adj} = 0.64, n=31). This model demonstrated that
328 mean values increased with the previous summer's average Chl *a* concentrations

and the duration of ice cover, but declined with spring water temperature (Fig. 4a-c), and was comparable when only open-water spring pCO_2 was considered (77.5% deviance explained, data not shown). In contrast, GAMs were significant, but less predictive for both mean summer and fall pCO_2 values. In these models, mean summer pCO_2 declined with increases in mean summer Chl *a* concentrations, but tended to increase with pCO_2 recorded the previous spring, particularly at high values (Fig. 4d-e, 43.6% deviance explained, $R^2_{adj} = 0.4$, n = 36). Similarly, fall pCO_2 declined with elevated autumnal Chl *a* concentrations, but showed more complex (unimodal) relationships with both summer pCO_2 and water temperature during fall (Fig. 4f-h, 23.3% deviance explained, $R^2_{adj} = 0.28$, n= 34). DOC was not a significant predictor and did not end up in any final model.

Discussion

Weekly estimates of CO_2 content of Buffalo Pound lake over 36 years demonstrated that a eutrophic hardwater lake could remain a net source of CO_2 to the atmosphere (Fig. 1) despite elevated algal production and pH (Finlay et al. 2009, 2015). However, we found clear evidence of legacy effects in all seasons (Fig. 4). Specifically, GAMs suggested that spring CO_2 content and efflux rates were derived mainly from winter metabolism of organic matter produced the previous summer, with longer ice-cover duration serving to increase both factors (Kratz et al. 1987; Baehr and DeGrandpre 2004). While CO_2 effluxes were lower during summer and fall than in spring (Fig. 3), pCO_2 values in summer and fall were also regulated by

interactions between current lake production and the legacy of the previous season's CO_2 concentration. Overall, we found no evidence of a major release of CO_2 during fall, as often occurs in thermally stratified lakes (Cole et al. 1994; Hesslein et al. 1991; Ducharme-Riel et al. 2015) and conclude that annual CO_2 budgets are strongly influenced by spring efflux, and therefore antecedent limnological conditions (Fig. 4). Given the highly synchronous patterns in CO_2 and other limnological parameters of lakes in this region (Vogt et al. 2011; Finlay et al. 2015), we believe that these results will be representative of other lakes in the Northern Great Plains (e.g., Meding and Jackson 2003; Maheux et al. 2016; Donald et al. 2015).

Temporal variation in CO_2

Total CO_2 flux in spring strongly influenced the magnitude of annual CO_2 flux in Buffalo Pound owing to elevated respiratory derived CO_2 under ice. Total spring efflux of CO_2 averaged 9.69 mol CO_2 m^{-2}, which is comparable to that observed in DOC-rich Wisconsin and Finnish lakes (1.1-13.7 mmol CO_2 m^{-2} $spring^{-1}$, Striegl et al. 2001), whereas vernal open-water release alone was 32.9 $\pm$ 19.8% of annual values. Summer pCO_2 remained relatively low and, with the exception of a few anomalous years, there was little indication of hypolimnetic CO_2 release in fall (Vachon and del Giorgio 2014; Ducharme-Riel et al. 2015). Mean fall values for pCO_2 and CO_2 flux were only slightly higher than in summer, consistent with the polymictic status of Buffalo Pound and the irregular occurrence of thermal stratification during summer (Dröscher et al. 2009). In general, Buffalo Pound lake was a net annual source of CO_2 to the atmosphere, with mean total annual flux of CO_2 (18.53 mol m^{-2} $year^{-1}$)

and mean daily flux rates (103.95 mmol m^{-2} day^{-1}), comparable to other hard-water systems (Striegl and Michmerhuizen 1998) but higher than boreal lakes (Rantakari and Kortelainen 2005; Abnizova et al 2012; Ducharme-Riel et al. 2015).

Atmospheric exchange of CO_2 during spring accounted for 63.8% of annual CO_2 efflux from Buffalo Pound Lake, a value much higher than that found elsewhere (Anderson et al. 1999; Ducharme-Riel et al. 2015) and reported earlier for this site (Finlay et al. 2015). However, this result includes both the "potential" and "open-water" spring fluxes and assumes both that ice is highly permeable to gas exchange prior to its complete disappearance, and that CO_2 efflux to the atmosphere is the main mechanism reducing CO_2 content during spring. If instead, gas exchange is limited through even fully-fractured ice due to limited hydrologic and atmospheric exchange (Loose et al. 2011) and degassing occurs following formation of marginal (lateral) open water immediately prior to full ice melt (Loose and Schlosser 2011), then CO_2 efflux declines to ca. 33% of annual flux, a value more in line with boreal systems. Further, we note that CO_2 could have declined under ice in Buffalo Pound due to alternate mechanisms, including elevated primary production by attached and motile algae (Salmi and Salonen 2016; Hampton et al. 2016), redistribution of CO_2-rich deepwaters by convective water-column currents (Kelley 1997; Mironov et al. 2002; Pernica et al. 2017), or chemical dissolution of sedimentary $CaCO_3$ (Finlay et al. 2015). Taken together, these observations suggest that our spring estimates represent the maximum possible CO_2 efflux, and illustrate that intensive studies of under-ice processes in the weeks prior to ice melt are needed to fully characterize the magnitude and importance of vernal CO_2 release.

Here, our GAM analyses reaffirmed that warmer winters with reduced ice-cover duration results in lower winter CO_2 accumulation and thus emissions in spring, as has been observed previously (Finlay et al. 2009, 2015). We did not, however, see similar consistent decadal trends for annual or seasonal CO_2 flux. In part, these differences arise because the duration of ice cover declined during the most recent 20-year interval studied by Finlay et al. (2015), but not during the entire 36-year period included here ($r^2 = -0.01$, $p = 0.5$). Given the elevated contribution of spring CO_2 fluxes to the annual budgets, as seen here and in other lake districts (Kratz et al. 1987; Cole et al. 1994; Striegl and Michmerhuizen 1998), climate change is likely to profoundly alter future lake CO_2 fluxes. Specifically, future prairie climates will be warmer and drier (Sauchyn and Kulshreshtha 2008; Lapp et al. 2009; Newton et al. 2014), with less ice cover (Shuter et al. 2013), patterns that should reduce the magnitude of CO_2 emissions in spring. This reduced spring CO_2 flux will translate into a reduction of long-term annual flux provided there is an alternative loss pathway for this C, such as carbonate precipitation or organic matter sedimentation (Tranvik et al. 2009), both of which are common in productive, hard-water lakes. Although reduced ice cover can potentially affect annual primary production, we found no significant relationship between ice duration and summer Chl *a* ($r^2 = 0.061$, $p = 0.15$) during the past 36 years when ice cover varied from 133 to 183 days. Instead, given that regional phytoplankton biomass is a complex function of temperature and nutrient influx (Vogt et al. 2018), and given the legacy effects seen herein, we infer that further changes in spring and

418 annual CO_2 emissions will also depend heavily on the effectiveness of nutrient
419 management strategies (Leavitt et al. 2006; Bunting et al. 2016).

420 *Controls of seasonal pCO_2*

421 Controls of CO_2 content and potential atmospheric exchange were strongly
422 influenced by lake production but differed in form and function among seasons.
423 During spring, pCO_2 was strongly and positively influenced by mean Chl *a* content of
424 the previous summer, consistent with microbial respiration of autochthonous
425 organic matter consuming oxygen (Meding and Jackson 2003; Powers et al. 2017)
426 and producing CO_2 (Kratz et al. 1987; Finlay et al. 2015) under ice. While pCO_2
427 levels in spring were also enhanced by the duration of ice cover (longer time for CO_2
428 accumulation) and cool spring temperatures (enhanced gas solubility), the
429 paramount effect of Chl *a* may reflect the highly eutrophic conditions in Buffalo
430 Pound (Hall et al. 1999; McGowan et al. 2005). Although present at elevated
431 concentrations, allochthonous DOC in Buffalo Pound is recalcitrant relative to other
432 sources (Williamson et al. 1999; Guillemette et al. 2017), largely unrelated to rates
433 of microbial production (Finlay et al. 2010), and was not included in our final
434 models of CO_2 content. Instead, it appears that factors regulating mid-summer
435 production may be unanticipated but important controls of subsequent spring CO_2
436 efflux.

437 GAMs also suggested that coeval Chl *a* was correlated negatively with pCO_2
438 during in both summer and fall, consistent with a strong role of phytoplankton
439 uptake during photosynthesis as seen in other autotrophic lakes (del Giorgio and

440 Peters 1994). Additional influences of microbial processes are indicated also by the
441 presence of a positive relationship between temperature and pCO_2 in fall, a pattern
442 consistent with the role of bacterial respiration of OM (del Giorgio and Peters 1994;
443 Cole et al. 2000), rather than changes in gas solubility as the lake cools (Pinho et al.
444 2016). Again, we were unable to detect an effect of DOC on pCO_2 from Buffalo
445 Pound in either summer or fall models, possibly because groundwater inputs,
446 carbonate buffering, calcification, and anaerobic metabolism also decouple the
447 relationship between allochthonous DOC influx and microbial metabolism in
448 regional lakes (Bogard and del Giorgio 2016; Stets et al. 2017). Full carbon budgets
449 in each season, including catchment loading of organic and inorganic carbon, would
450 be required in order to fully evaluate these alternatives.

451 *Legacy effects of climate and limnological conditions*

452 Analysis of a 36-year continuous time series of water chemistry
453 demonstrated that instantaneous estimates of CO_2 content in lake waters are
454 regulated by current limnological conditions as well as the persistent influence of
455 lake conditions in earlier seasons. Such legacy effects are well known from studies
456 of terrestrial biogeochemistry (Cuddington 2011) and land-water linkages (Martin
457 et al. 2011), but are less well understood for in situ biogeochemical cycles (Meding
458 and Jackson 2003; Hampton 2015). Recent studies suggest that spring water
459 chemistry is strongly influenced by under-ice processes (Powers et al. 2017) and,
460 consistent with that view, our GAM analysis showed that vernal pCO_2 could be
461 predicted best (72.6% of deviance explained) from a combination of mean Chl *a*

462 concentration during the previous summer, ice-cover duration during the
463 antecedent winter, and coeval spring water temperature. Overall, historical
464 parameters had a paramount effect on spring model performance (Fig. 4), while
465 coeval biological parameters were non-significant (e.g., spring Chl *a*), suggesting
466 that vernal CO_2 fluxes were controlled mainly by limnological and climatic
467 conditions in earlier seasons. Given the potential importance of spring CO_2 efflux to
468 the annual CO_2 budgets (see above), these findings suggest that atmospheric
469 warming (Finlay et al. 2015) and surface-water eutrophication (Leavitt et al. 2006;
470 Bunting et al. 2016) will interact in complex manners to regulate the importance of
471 hardwater lakes in global carbon budgets.

472 Comparison of GAMs developed for individual seasons demonstrates that the
473 strength of legacy effects declines continuously through the ice-free period, both in
474 terms of explanatory power and the influence of historical parameters on gas fluxes
475 (Fig. 4). Specifically, the predictive power of GAMs declined by ~50% in successive
476 seasons, from spring (72.6%) to summer (43.6%) and fall (23.3%), while only pCO_2
477 levels during the preceding season were retained as a secondary predictor in
478 summer and fall models. Although speculative, we infer that these declines may
479 reflect the progressive accumulation of effects of intervening meteorological events
480 (e.g., wind, low pressure cells, etc.) which are known to influence CO_2 fluxes at the
481 scale of days to weeks (Morales-Pineda et al. 2014). In addition, as coeval Chl *a*
482 concentrations were retained in latter models, yet are strongly influenced by
483 summer water temperatures and nutrient content in Buffalo Pound and other
484 regional lakes (Vogt et al. 2018), we infer that immediate controls of these

485 limnological parameters may override the importance of legacy effects on CO_2
486 content and flux.

487 **Conclusion**

488 These analyses used a 36-year time series with weekly resolution from a
489 hard-water lake to demonstrate that instantaneous pCO_2 is regulated by a
490 combination of current limnological conditions and legacy effects from earlier
491 seasons. This legacy effect was most pronounced in spring and declined throughout
492 the ice-free season. The form and identity of physico-chemical controls also
493 changed through time, with climate (ice-cover duration) being strongest predictor
494 in spring model, and coeval estimates of lake metabolism (Chl *a*) mainly regulating
495 pCO_2 in summer and fall. The strength of these relationships reflects our ability to
496 predict CO_2 in the future. Specifically, the strong spring relationship suggests that
497 future climate warming and reduction of ice cover will diminish the importance of
498 antecedent conditions, and may reduce annual CO_2 emissions to the atmosphere,
499 particularly if efforts to reduce nutrient loading in this region are successful. This
500 relationship explained 72% of the variability in the data, which allows for
501 predictions of how future climate change will affect lake carbon processing in this
502 system.

503

504 **References**

505 Abnizova, A., J. Siemens, M. Langer, and J. Boike. 2012. Small ponds with major
506 impact: The relevance of ponds and lakes in permafrost landscapes to carbon

dioxide emissions. Global Biogeochem. Cycles. **26** GB2041. doi:10.1029/2011GB004237

Anderson, D. E., R. G. Striegl, D.I. Stannard, C. M. Michmerhuizen, T.A. McConnaughey, and J. W. LaBaugh. 1999. Estimating lake-atmosphere CO_2 exchange. Limnol. Oceanogr. **44**: 988–1001, doi:10.4319/lo.1999.44.4.0988

Baehr, M. M., and M. D. DeGrandpre. 2002. Under-ice CO_2 and O_2 variability in a freshwater lake. Biogeochemistry. **61**: 95-113.

Baehr, M. M., and M. D. DeGrandpre. 2004. In situ pCO_2 and O_2 measurements in a lake during turnover and stratification: Observations and modeling. Limnol. Oceanogr. **49**: 330–340. doi: 10.4319/lo.2004.49.2.0330.

Bogard, M. J., and P. A. del Giorgio. 2016. The role of metabolism in modulating CO_2 fluxes in boreal lakes. Global Biogeochem. Cycles. **30**: 1509–1525. doi: 10.1002/2016GB005463.

Bunting, L., P. R. Leavitt, G. L. Simpson, B. Wissel, K. R. Laird, B. F. Cumming, A. St. Amand, and D. R. Engstrom. 2016. Increased variability and sudden ecosystem state change in Lake Winnipeg, Canada, caused by 20th century agriculture. Limnol. Oceanogr. **61**: 2090–2107. doi: 10.1002/lno.10355.

Cole, J. J., N. F. Caraco, G. W. Kling, T. K. Kratz. 1994. Carbon dioxide supersaturation in the surface waters of lakes. Science. **265**: 1569-1570. Doi: 10.1126/science.265.5178.1568.

Cole, J. J., and others. 2007. Plumbing the Global Carbon Cycle: Integrating Inland Waters into the Terrestrial Carbon Budget. Ecosystems, **10**: 172–185. doi:10.1007/s10021-006-9013-8.

530 Cuddington, K. 2011. Legacy effects: The persistent impact of ecological interactions.
531 Biol. Theory. **6**: 203-210. Doi: 10.1007/s13752-012-0027-5.
532 del Giorgio, P. A., and R. H. Peters. 1994. Patterns in planktonic P:R ratios in lakes:
533 Influence of lake trophy and dissolved organic carbon. Limnol. Oceanogr. **39**:
534 772–787. doi:10.4319/lo.1994.39.4.0772.
535 Denfeld, B. A., P. Kortelainen. M. Rantakari, S. Sobek, and G. A. Weyhenmeyer. 2015.
536 Regional variability and drivers of below ice CO_2 in boreal and subarctic lakes.
537 Ecosystems. **19**: 461–476. doi: 10.1007/s10021-015-9944-z.
538 Dillon, P. J., and L. A. Molot, L. A. 1997. Dissolved organic and inorganic carbon mass
539 balances in central Ontario lakes. Biogeochemistry. **36**: 29–42.
540 doi:10.1023/A:1005731828660.
541 Donald, D. B., B. R. Parker, J.-M. Davies, and P. R. Leavitt. 2015. Nutrient
542 sequestration in the Lake Winnipeg watershed. J. Great Lakes Res. **41**: 630-642.
543 Dröscher I., A. Patoine, K. Finlay, and P.R. Leavitt. 2009. Climate control of the spring
544 clear-water phase through the transfer of energy and mass to lakes. Limnol.
545 Oceanogr. **54**: 2469-2480
546 Ducharme-Riel, V., D. Vachon, P. A. del Giorgio, and Y. T. Prairie. 2015. The relative
547 contribution of winter under-ice and summer hypolimnetic CO_2 accumulation to
548 the annual CO_2 emissions from northern lakes. Ecosystems. **18**: 1–13. doi:
549 10.1007/s10021-015-9846-0.
550 Finlay, K., P. R. Leavitt, B. Wissel, and Y. T. Prairie. 2009. Regulation of spatial and
551 temporal variability of carbon flux in six hard-water lakes of the northern Great
552 Plains. Limnol. Oceanogr. **54**: 2553-2564.

553 Finlay, K., P. R. Leavitt, A. Patoine, and B. Wissel. 2010. Magnitudes and controls of
554 organic and inorganic carbon flux through a chain of hard-water lakes on the
555 northern Great Plains. Limnol. Oceanogr. **55**: 1551-1564. doi:
556 10.4319/lo.2010.55.4.1551
557 Finlay, K., R. J. Vogt, M. J. Bogard, B. Wissel, B. M. Tutolo, G. L. Simpson, and P. R.
558 Leavitt, 2015. Decrease in CO_2 efflux from northern hardwater lakes with
559 increasing atmospheric warming. Nature, **519**: 1–13. doi: 10.1038/nature14172
560 Gerten, D., and R. Adrian. 2000. Climate-driven changes in spring plankton dynamics
561 and the sensitivity of shallow polymictic lakes to the North Atlantic Oscillation.
562 Limnol. Oceanogr. **45**: 1058–1066. doi: 10.4319/lo.2000.45.5.1058
563 Guillemette, F. O., E. von Wachenfeldt, D. N. Kothawala, D. Bastviken, and L. J.
564 Tranvik, L. J. 2017. Preferential sequestration of terrestrial organic matter in
565 boreal lake sediments. J. Geophys. Res: *Biogeosciences*. **122**: 863–874. doi:
566 10.1002/2016JG003735.
567 Hall, R. I., P. R. Leavitt, and A. S. Dixit 1999. Limnological succession in reservoirs: A
568 paleolimnological comparison of two methods of reservoir formation. Can J. Fish.
569 Aquat. Sci. **56**: 1109–1121. doi: 10.1139/f99-047.
570 Hammer, U. T. 1986. Saline lake ecosystems of the world. Junk.
571 Hampton, S. E., and others. 2016. Ecology under lake ice. Ecology Letters.,**20**: 98–
572 111. doi:10.1111/ele.12699.
573 Hesslein R. H., J. W. M. Rudd, C. Kelly, P. Ramlal, and K. A. Hallard. 1991. Carbon
574 dioxide pressure in surface waters of Canadian lakes. In: Wilhelms S.C. and
575 Gulliver J.S. (eds), Air-water mass transfer., pp. 413-43. Am. Soc. Civil Eng.

576 Hoover, T. E., and D. C. Berkshire. 1969. Effects of hydration on carbon dioxide
577 exchange across an air-water interface. J. Geophys. Res. **74**: 456-464.
578 Kelley, D. E. 1997. Convection in ice-covered lakes: Effects of algal suspension. J.
579 Plankton Res. **19**: 1859-1880.
580 Kratz, T. K., R. B. Cook, and C. J. Bowser. 1987. Winter and spring pH depressions in
581 northern Wisconsin lakes caused by increases in pCO_2. Can. J. Fish. Aquat. Sci. **44**:
582 1082-1088.
583 Lapp, S., D. Sauchyn, and B. Toth. 2009. Constructing scenarios of future climate and
584 water supply for the SSRB: use and limitations for vulnerability assessment.
585 Prairie Forum **34**: 153–180.
586 Leavitt, P. R., C. S. Brock, C. Ebel, and A. Patoine. 2006. Landscape-scale effects of
587 urban nitrogen on a chain of freshwater lakes in central North America. Limnol.
588 Oceanogr. **51**: 2262–2277.
589 Loose, B., and P. Schlosser. 2011. Sea ice and its effect on CO2 flux between the
590 atmosphere and the Southern Ocean interior. J. Geophysical Res. Oceans. **116**:
591 C11019. doi:10.1029/2010JC006509.
592 Loose, B., P. Schlosser, D. Perovich, D. Ringelberg, D. T. Ho, T. Takahashi, J. Richter-
593 Menge, C. M. Reynolds, W. R. Mcgillis, and J.-L. Tison. 2011. Gas diffusion through
594 columnar laboratory sea ice: Implications for mixed-layer ventilation of CO_2 in
595 the seasonal ice zone. Tellus B: Chem. Phys. Meteorol. **63**: 23-39, doi:
596 10.1111/j.1600-0889.2010.00506.x
597 López Bellido, J., T. Tulonen, P. Kankaala, P. and A. Ojala. 2012. Concentrations of CO_2
598 and CH_4 in water columns of two stratified boreal lakes during a year of atypical

summer precipitation. Biogeochemistry. **113**: 613–627. doi: 10.1007/s10533-012-9792-2

Maberly, S. C. 1996. Diel, episodic and seasonal changes in pH and concentrations of inorganic carbon in a productive lake. Freshwat. Biol. **35**: 579–598. doi: 10.1111/j.1365-2427.1996.tb01770.x

Maheaux, H., P. R. Leavitt, and L. J. Jackson. 2016. Asynchronous onset of eutrophication among shallow prairie lakes of the northern Great Plains, Alberta, Canada. Global Change Biol. **22**: 271–283.

Martin, S.L., D.B. Hayes, D.T. Rutledge, and D.W. Hyndman. 2011. The land-use legacy effect: Adding temporal context to lake chemistry. Limnol. Oceanogr. **56**: 2362-2370. Doi:10.4319/lo.2011.56.6.2362.

McGowan, S., P. R. Leavitt, and R. I. Hall. 2005. A whole-lake experiment to determine the effects of winter droughts on shallow lakes. Ecosystems **7**: 694-708.

Meding, M. E., and L. J. Jackson. 2003. Biotic, chemical and morphometric factors contributing to winter anoxia in prairie lakes. Limnol. Oceanogr. **48**: 1633-1642.

Mironov, D., A. Terzhevik, G. Kirillin, T. Jonas, J. Malm, and D. Farmer. 2002. Radiatively driven convection in ice-covered lakes: Observations, scaling, and a mixed layer model. J. Geophys. Res. **107**: C4, 3032. doi: 10.1029/2001JC000892.

Morales-Pineda, M., Cózar, A., Laiz, I., Úbeda, B., & Gálvez, J. Á. (2014). Daily, biweekly, and seasonal temporal scales of pCO_2 variability in two stratified Mediterranean reservoirs. J. Geophys. Res: Biogeosci. **119**: 509–520. doi: 10.1002/2013JG002317

622 Newton, B. W., T. D. Prowse, and B. R. Bonsal. 2014. Evaluating the distribution of
623 water resources in western Canada using synoptic climatology and selected
624 teleconnections. Part 2: summer season. Hydrol. Process.. **28**: 4235–4249.
625 doi:10.1002/hyp.10235.
626 Pernica, P., R. L. North, and H. M. Baulch. 2017. In the cold light of day: The potential
627 importance of under-ice convective mixed layers to primary producers. Inland
628 Wat. **7**: 138–150. doi:10.1080/20442041.2017.1296627.
629 Pinho, L., C. M. Duarte, H. Marotta, and A. Enrich-Prast. 2016. Temperature
630 dependence of the relationship between pCO_2 and dissolved organic carbon in
631 lakes. Biogeosciences **13**: 865–871. doi:10.5194/bg-13-865-2016.
632 Powers, S. M., S. G. Labou, H. M. Baulch, R. J. Hunt, N. R. Lottig, S. E. Hampton, and E.
633 H. Stanley. 2017. Ice duration dries winter nitrate accumulation in north
634 temperate lakes. Limnol. Oceanog. Letts. **2**: 177-189. doi: 10.1002/lol2.10048
635 Prairie, Y. T. 2008. Carbocentric limnology: looking back, looking forward. Can. J.
636 Fish. Aquat. Sci. **65**: 543–548. doi:10.1139/f08-011.
637 Pya, N., and S. N. Wood. 2016. February 22. A note on basis dimension selection in
638 generalized additive modelling. arXiv [stat.ME]. Retrieved from
639 http://arxiv.org/abs/1602.06696

640 R Core Team. 2017. R: A language and environment for statistical computing. R
641 Foundation for Statistical Computing, Vienna, Austria. URL https://www.R-
642 project.org/.

643 Rantakari, M., and P. Kortelainen. 2005. Interannual variation and climatic
644 regulation of the CO_2 emission from large boreal lakes. Glob. Change Biol. **11**:
645 1368–1380. doi:10.1111/j.1365-2486.2005.00982.x.
646 Salmi, P., and K. Salonen. 2015. Regular build-up of the spring phytoplankton
647 maximum before ice-break in a boreal lake. Limnol. Oceanogr. **61**: 240–253. Doi:
648 10.1002/lno.10214
649 Sauchyn D., and S. Kulshreshtha. 2008. The Prairies. From impacts to adaptation:
650 Canada in a changing climate. Government of Canada, Ottawa
651 Shuter, B. J., C. K. Minns, and S. R. Fung. 2013. Empirical models for forecasting
652 changes in the phenology of ice cover for Canadian lakes. Can. J. Fish. Aquat. Sci.
653 **70**: 982–991. doi: 10.1139/cjfas-2012-0437.
654 Stets, E. G., R. G. Striegl, G. R. Aiken, D. O. Rosenberry, and T. C. Winter. 2009.
655 Hydrologic support of carbon dioxide flux revealed by whole-lake carbon
656 budgets. J. Geophys. Res. **114**(G1): G01008–14. doi:10.1029/2008JG000783
657 Stets, E. G., D. Butman, C. P. McDonald, S. M. Stackpoole, M. D. DeGrandpre, and R. G.
658 Striegl. 2017. Carbonate buffering and metabolic controls on carbon dioxide in
659 rivers. Global Biogeochem. Cycles. **31**: 663–677. doi: 10.1002/2016GB005578.
660 Striegl, R. G., P. Kortelainen, J. P. Chanton, K. P. Wickland, G. C. Bugna, and M.
661 Rantakari. 2001. Carbon dioxide partial pressure and ^{13}C content of north
662 temperate and boreal lakes at spring ice melt. Limnol. Oceanogr. **46**: 941–945.
663 doi:10.4319/lo.2001.46.4.0941.

664 Striegl, R. G., and C. M. Michmerhuizen. 1998. Hydrologic influence on methane and
665 carbon dioxide dynamics at two north-central Minnesota lakes. Limnol.
666 Oceanogr. **43**: 1519–1529. doi: 10.4319/lo.1998.43.7.1519.
667 Tranvik, L. J., J. A., Downing, J. B. Cotner, S. A. Loiselle, R. G. Striegl, T. J. Ballatore, P.
668 Dillon, K. Finlay, and others. 2009. Lakes and reservoirs as regulators of carbon
669 cycling and climate. Limnol. Oceanogr. **54**: 2298–2314. doi:
670 10.4319/lo.2009.54.6_part_2.2298.
671 Vachon, D. and Y. T. Prairie. 2013. The ecosystem size and shape dependence of gas
672 transfer velocity versus wind speed relationships in lake. Can. J. Fish. Aquat. Sci. **70**:
673 1757-1764. doi:10.1139/cjfas-2013-0241
674 Vachon, D., and P. A. del Giorgio. 2014. Whole-Lake CO_2 Dynamics in response to
675 storm events in two morphologically different lakes. Ecosystems. **17**: 1338–
676 1353. doi:10.1007/s10021-014-9799-8.
677 Vogt, R. J., J. A. Rusak, A. Patoine, and P. R. Leavitt. 2011. Differential effects of energy
678 and mass influx on the landscape synchrony of lake ecosystems. Ecology. **92**:
679 1104-1114.
680 Vogt, R. J., S. Sharma, and P. R. Leavitt. 2018. Direct and interactive effects of climate,
681 meteorology, river hydrology, and lake characteristics on water quality in
682 productive lakes of the Canadian Prairies. Can. J. Fish. Aquat. Sci. **75**: 47–59. doi:
683 10.1139/cjfas-2016-0520.
684 Wetzel, R. G. 2001. Limnology. Academic Press.

685 Wickham, H. 2009. ggplot2: Elegant graphics for data analysis. Springer-Verlag New
686 York.
687 Williamson, C. E., D. P. Morris, M. L. Pace, and O. G. Olson. 1999. Dissolved organic
688 carbon and nutrients as regulators of lake ecosystems: Resurrection of a more
689 integrated paradigm. Limnol. Oceanogr. **44**: 795-803.
690 Winder, M., and D. E. Schindler. 2004. Climatic effects on the phenology of lake
691 processes. Global Change Biol. **10**: 1844–1856. doi: 10.1111/j.1365-
692 2486.2004.00849.x
693 Wood, S. N., N. Pya, and B. Säfken. 2016. Smoothing parameter and model selection
694 for general smooth models. J. Am. Stat. Assoc. **111**: 1548–1563.
695 doi:10.1080/01621459.2016.1180986
696 Wood, S. N. 2017. Generalized Additive Models: An introduction with R, Second
697 Edition. CRC Press. Boca Raton.
698
699

Acknowledgements

We thank Dan Conrad from the Buffalo Pound Water Treatment Plant in Moose Jaw, SK, for providing the water chemistry data. Emma Wiik helped collate the data and contributed to discussions regarding the analyses. Funding for this project was provided by an NSERC Discovery Grants to KF, GS and PRL. We acknowledge this research was conducted on Treaty 4 territory. This is a contribution to the Qu'Appelle long-term ecological research program (QU-LTER).

Figure Legends

Fig. 1 Total annual CO_2 flux in Buffalo Pound from 1979-2014, broken down by contribution by each open-water season. Spring is divided into "potential spring", the period between maximum pCO_2 and the ice-off date (black bars), and open-water spring", the period between ice-off and minimum pCO_2 (dark grey bars). Summer and fall are represented by medium and light grey bars, respectively. Flux is calculated using summed calculated CO_2 flux based on weekly data, extrapolated to 7 days. Winter flux under ice was considered to be zero.

Fig 2. Seasonally averaged pCO_2 by year of study in Buffalo Pound. No directional trends were observed for any season over the 36-year period.

Fig. 3. a) Generalized additive model of pCO_2 by year and day of year in Buffalo Pound based on 36 years of weekly data. Line colour represents year of sampling and shows little evidence of directional change in lake pCO_2 in the 36-year sampling period. b) GAM model as represented in a), but separated by year. Vertical lines

722 indicate ice-off and ice-on dates. Most years demonstrate a consistent pattern of
723 increasing pCO_2 under ice in winter, followed by efflux in spring, low pCO_2 in
724 summer and fall, and then CO_2 accumulation under ice in fall.

725 Fig. 4. Generalized additive model results for seasonally averaged pCO_2 in Buffalo
726 Pound. Spring average pCO_2 was best explained with a combination of a) chorophyll
727 a concentration in the previous summer, b) ice cover duration, and c) current water
728 temperature (GAM deviance explained = 72.6%), while summer average pCO_2 was
729 explained using d) current summer chlorophyll a concentration and e) average pCO_2
730 in the preceding spring (deviance explained = 43.6%), and fall was best explained
731 using f) current fall chlorophyll a concentration, g) preceding summer pCO_2 and h)
732 current fall water temperature (deviance explained = 23.3%). Plots are partial pots
733 of the smooth terms in the model, and the y axis is the intercept plus the partial
734 effect of the individual smooths.

735

736

737

738

739

740

741

742

743

744 Fig. 1

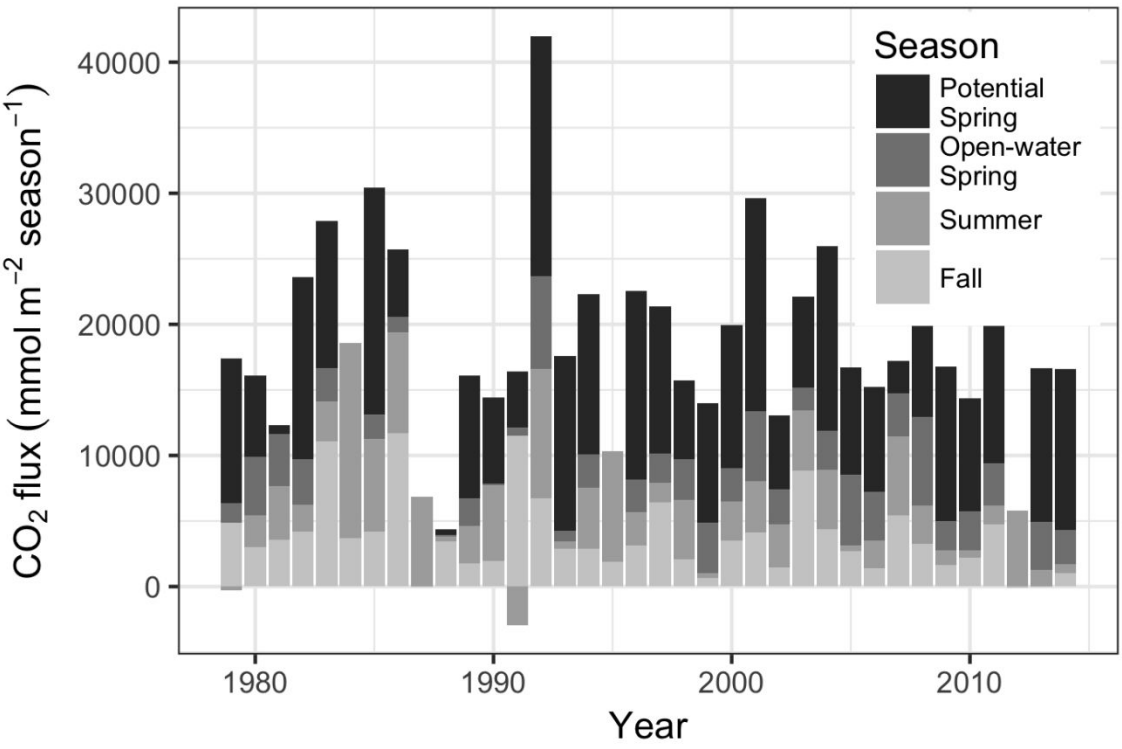

745

746

747

748 Fig. 2a

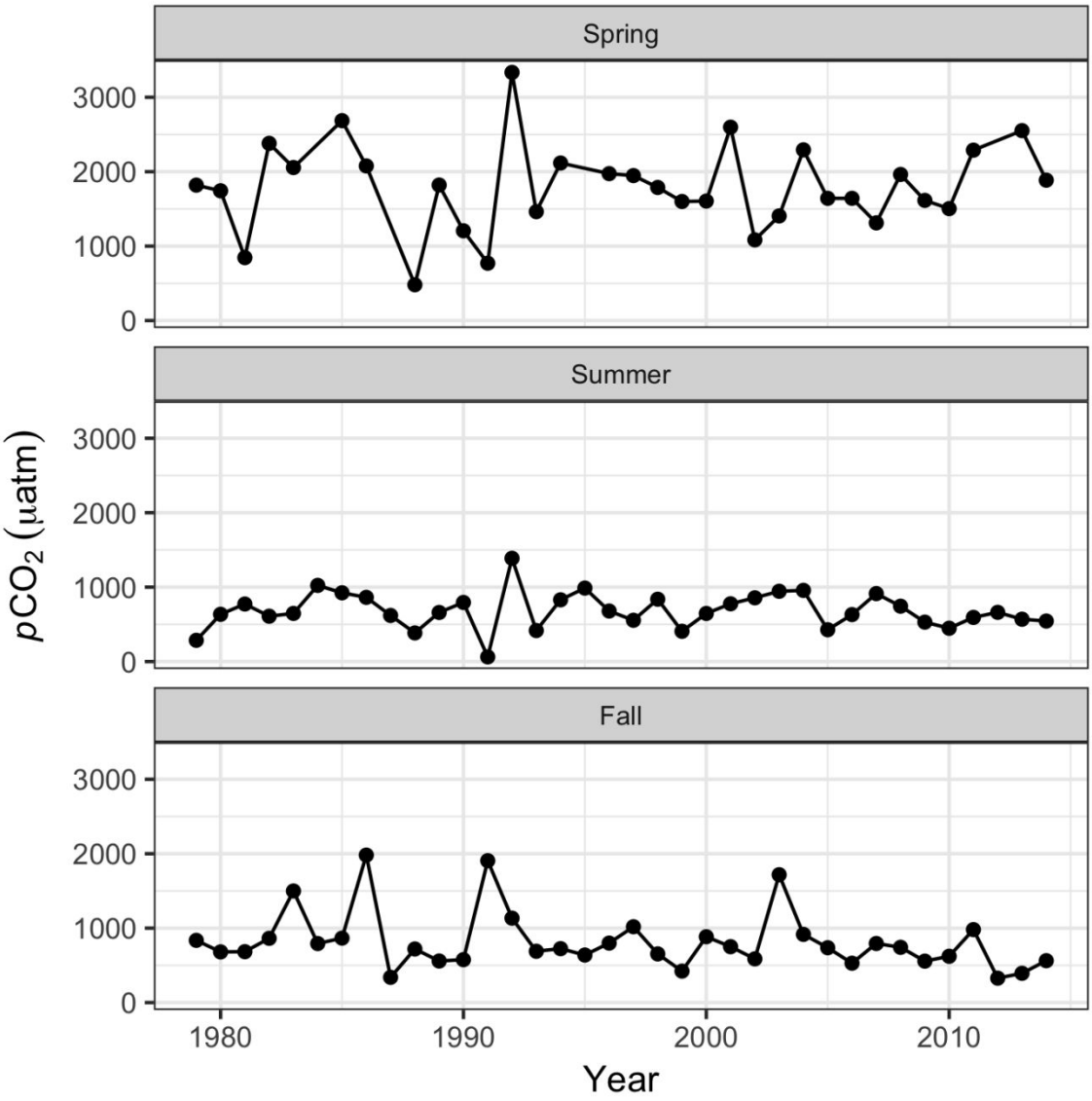

749

750

751

752

753

754

755

756

757

Fig. 3a)

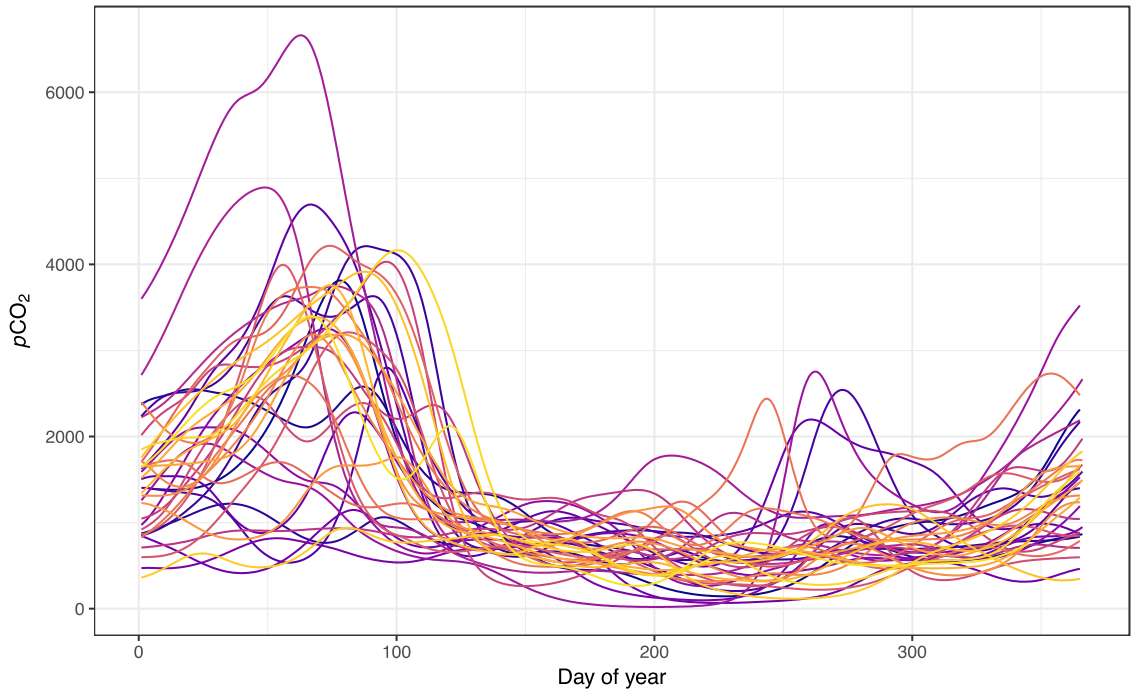

Fig. 3b)

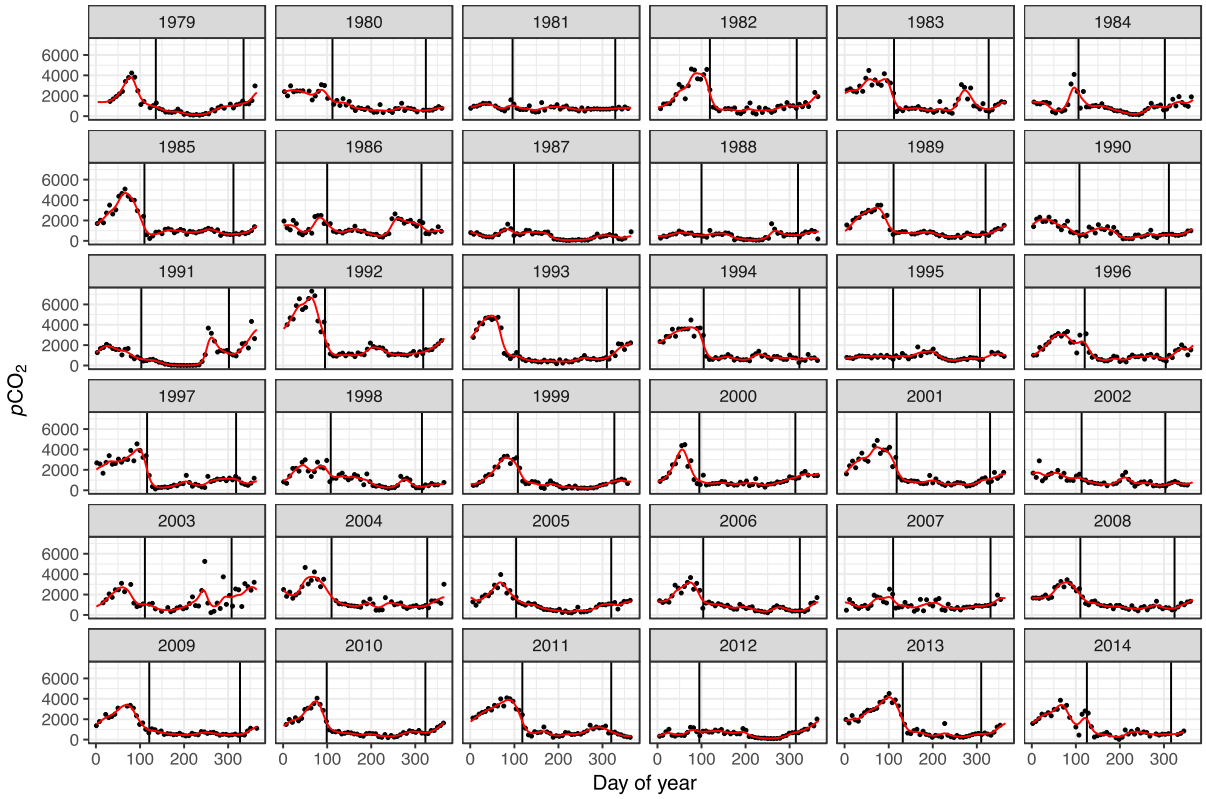

773
774
775
776
777
778
779
780
781
782
783
784
785

786 Fig. 4

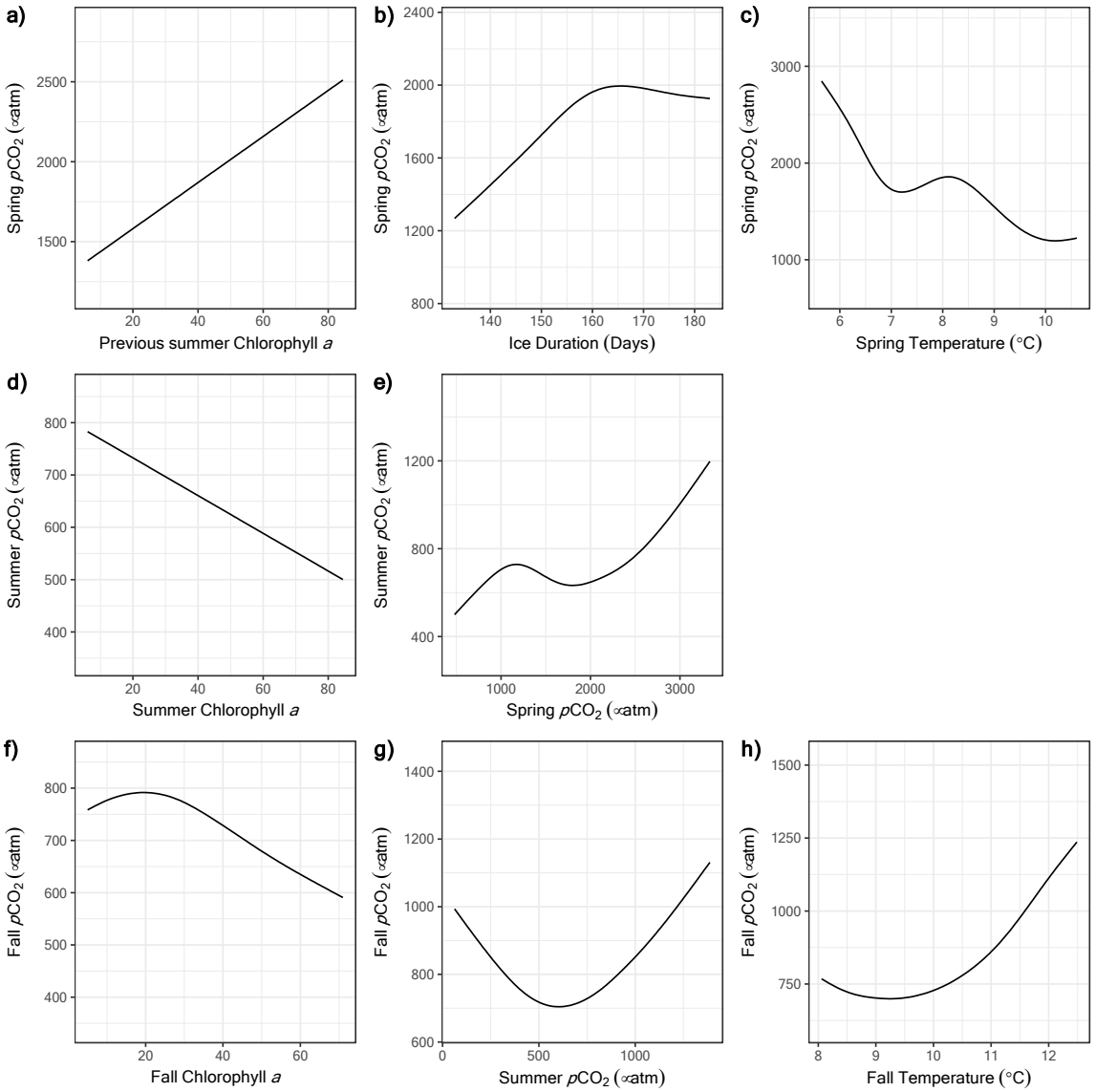

787

788

789 Supplementary Information

790 *GAM model selection and estimates*

791 Several candidate model forms were fitted to the data, which reflect slightly
792 different hypotheses as to the nature of the within- and between-year trends in the
793 pCO_2 record. Models estimated included i) additive within- and between-year
794 trends, ii) smoothly-varying interaction models where the within-year trend varies
795 as a smooth function of the between-year trend, iii) functional within-year trends,
796 where a separate seasonal effect is estimated for each year with the long-term trend
797 being modeled via a year random effect, and iv) complex smooth trends without a
798 separate within-year term. Where present in a candidate model, within-year trends
799 were estimated using cyclic cubic regression splines to avoid discontinuities
800 between weeks 52 (53) and 1 in adjacent years. Between-year trends were typically
801 modeled via thin plate splines, however, in one candidate model, an adaptive B
802 spline basis was used to allow the wiggliness of the long-term trend to vary as a
803 function of time; this possibility allows for periods of rapid and more complacent
804 change in pCO2 rather than the expectation of constant smoothness assumed by the
805 other model candidates. Models with interactions between the within- and between-
806 year trends were implemented using tensor products of cyclic cubic regression and
807 thin plate spline marginal bases.

808 In all cases, candidate models were estimate using maximum likelihood-
809 based smoothness selection procedures (Wood et al 2017). We used the Tweedie
810 distribution as the conditional distribution of pCO_2. This family of distributions has

811 support on the non-negative real numbers and as a result is suitable for modeling
812 the non-negative continuous pCO_2 data. This family also includes the gamma
813 distribution as a special case (when the power parameter, *p*, is 2), which is often
814 used to model positive, continuous data. In our models, the estimated value of the
815 power parameter was approximately p=1.5, indicating a weaker mean-variance
816 relationship than that of the gamma distribution. Using the procedure of (Pya &
817 Wood, 2016) the adequacy of the initial basis dimension of each smooth was
818 checked and, if deemed insufficient, a larger initial basis size was used and the
819 model refitted. The best-fitting model among the selection described above was
820 determined using a combination of AIC and qualitative exploration of the model fits.
821 For example, qualitative inspection indicated that the functional within-year trends
822 model resulted in discontinuous fits between years, producing a poorer fit to the
823 pCO2 time series, which was reflected in the model's relatively higher AIC.

824 To include the uncertainty in the estimated pCO_2 trend, we simulated 10,000
825 trends from the posterior distribution of the fitted GAM. Each of these simulated
826 trends is consistent with the estimated trend, but includes the effect of the
827 uncertainty in the estimates of the spline coefficients. Under the empirical Bayesian
828 formulation of the GAM, these coefficients are distributed mutlivariate normal with
829 estimated covariance matrix V (Wood, 2017). Hence our posterior simulation
830 involves drawing 10,000 samples from this multivariate normal distribution and
831 then application of the procedure to derive the difference between peak and
832 minimum pCO_2 for each sample (trend). The upper and lower 2.5th probability
833 quantiles of the distribution of the 10,000 differences in pCO_2 for each year form a

95% credible interval on the difference estimated from the fitted trend shown. Code to reproduce this analysis is available from https://github.com/simpson-lab/buffalo-pound-co2-ltpar-paper.

Model selection and output for controls of seasonal pCO_2

The final spring model included summer Chl a, current temp, and ice duration. All variables contributed significantly to the model, and their effects were comparable, with current spring temperature exerting the strongest effect.

This model has deviance explained = 72.6%, R^2adj = 0.64, n=31.

	Estimate	Estimated degrees of freedom	Reference degrees of freedom	p-value
Intercept	1796.3			<0.0001
Summer Chl a		1.285	9	<0.0001
Current Temp		4.021	9	<0.0001
Ice Duration		1.829	9	0.0023

Other candidate models included coeval (spring) Chl a, and DOC, however, the inclusion of these variables reduced the number of data points included in the model, and k was reduced to below 6 in order to get a fit. Consequently, these models had lower AIC, but explained deviance dropped to <50%.

The final model for summer pCO_2 included summer (current) Chl a and spring pCO_2. This model has deviance explained = 43.6%, R^2adj = 0.4, n=36.

	Estimate	Estimated degrees of freedom	Reference degrees of freedom	p-value

Intercept	685.1			<0.0001
Current Chl a		0.8443	9	0.0097
Spring pCO_2		3.4725	9	0.0011

850

851 Other candidate models examined the effect of Ice Duration and spring Chl a as
852 legacy effects. These additions reduced n, as above, and k was reduced down to 6.
853 Again, AIC was lowered in this alternate model, but deviance explained dropped to
854 <30%.

855 The fall model included current (fall) Chl a, summer pCO_2 and current (fall) temp.
856 This model has deviance explained = 23.3%, R^2adj = 0.28, n=34.

	Estimate	Estimated degrees of freedom	Reference degrees of freedom	p-value
Intercept	768.45			<0.0001
Current Chl a		0.936	9	0.0963
Summer pCO_2		1.736	9	0.0179
Temp		1.838	9	0.0019

857

858 Other candidate models included legacy effects by adding in Ice Duration and
859 summer Chl a, but the additional variables in the model required a reduction of k
860 down to 6, and deviance explained dropped to <15%.

861

862

863